# HIGH-RESOLUTION DETECTION OF MUSCLE CROSSBRIDGE ORIENTATION BY ELECTRON PARAMAGNETIC RESONANCE

VINCENT A. BARNETT, PIOTR FAJER, CARL F. POLNASZEK, AND DAVID D. THOMAS
*Department of Biochemistry, Medical School, University of Minnesota, Minneapolis, Minnesota 55455*

Skeletal muscle fibers consist of hexagonally packed actin and myosin filaments. According to x-ray diffraction and electron microscopy (EM), the structure is highly ordered both in hexagonal packing and along the filament axis. Globular actin monomers are organized in a double-stranded helix, while myosin molecules are stacked so that their elongated globular heads form a three-stranded helix. The attachment of the these heads to actin filaments, followed by their rotation, is thought to cause sliding of the filaments past each other and thus provide the molecular basis of muscle contraction. This hypothesis is consistent with x-ray and EM evidence indicating a high degree of order in rigor, i.e., in the absence of ATP, with the heads forming cross-bridges between the myosin and actin filaments (Huxley and Brown, 1967) and the absence of these ordered cross-bridges in relaxing media (Heuser, 1983; Poulsen and Lowy, 1983). Unfortunately, x-ray diffraction does not provide direct information about crossbridge orientation, and EM cannot be used in functional muscle fibers. More specific measurements of cross-bridge orientation in functional fibers can be provided by EPR spectroscopy, which is primarily sensitive to both the orientational distribution of site-specific spin labels and also to their rotational motion. In previous EPR studies of spin labels attached to cross-bridges in glycerinated muscle fibers, we have shown that in relaxed fibers the heads are dynamically disordered (executing large-amplitude microsecond motions) while in rigor the same heads are ordered and their motion is severely restricted (Thomas and Cooke, 1980; Thomas et al., 1980; Barnett and Thomas, 1984). The present work illustrates how the theory of conventional EPR lineshapes can be used quantitatively to determine the orientational distribution of spin labels attached to myosin heads.

## THEORY

Conventional EPR spectra were simulated as described by Thomas and Cooke (1980). To a good approximation, in the absence of submicrosecond rotational motion, the position at which a nitroxide spin label contributes to the absorption spectrum depends on only two variables: the nitrogen nuclear quantum number $m_I$ $(-1, 0, +1)$ and the quantity $\langle \hat{z} \cdot \hat{H}_0 \rangle^2 = \cos^2(\theta)$ where $\theta$ is the angle between the static magnetic field $\hat{H}_0$ and the principal axis $\hat{z}$ of the spin label:

$$H_{res}(\theta, m_I) = g_\parallel \hat{H}_0 / g(\theta) + m_I T(\theta)$$
$$g(\theta) = g_\parallel \cos^2\theta + g_\perp \sin^2\theta$$
$$T(\theta) = [T_\parallel^2 \cos^2\theta + T_\perp \sin^2\theta]^{1/2}. \quad (1)$$

This orientation dependence is illustrated by the simulated conventional EPR ($V_1$) spectra in the top row of Fig. 1. Thus for a uniformly oriented population of spin labels having a single value of $\cos^2\theta$ (e.g., in a single crystal, in a stack of crystalline membranes oriented normal to $H_0$, or in a bundle of perfectly helical fibers oriented parallel to the magnetic field), one observes a three-line spectrum in which the position of the center line is determined by $g(\theta)$ and the splitting between the three lines is determined by $T(\theta)$. Fig. 1 shows that each of these lines is so narrow that spectra corresponding to only slightly different orientations are easily resolved.

If there is only partial orientational order of the spin labels within a sample, the EPR spectrum provides a direct and unambiguous readout of the orientational distribution. That is, in contrast to optical spectroscopy, EPR provides independent information on the average orientation, the orientational disorder, and the number of discrete preferred orientations in the population. For example, Fig. 1 shows spectra corresponding to a spherically weighted Gaussian distribution of orientations $\rho(\theta)$ centered at $\theta_0$ and having a full width at half maximum of $\Delta\theta$:

$$\rho(\theta) = (\sin\theta) \exp[-(\ln 2)\{(\theta - \theta_0)/\Delta\theta/2]^2] \quad (2)$$

Each row in Fig. 1 demonstrates the sensitivity of the conventional EPR spectrum to changes in $\theta_0$. In each of the columns, the angular spread of orientations, $\Delta\theta$, is varied from perfect orientation ($\Delta\theta = 0°$) to a random distribution ($\Delta\theta > 180°$). Following the spectra in each column, we note that the lines become progressively broader (and less equal in height) with increasing angular spread ($\Delta\theta$). The splitting, however, remains essentially constant in each column, i.e., is independent of $\Delta\theta$. In

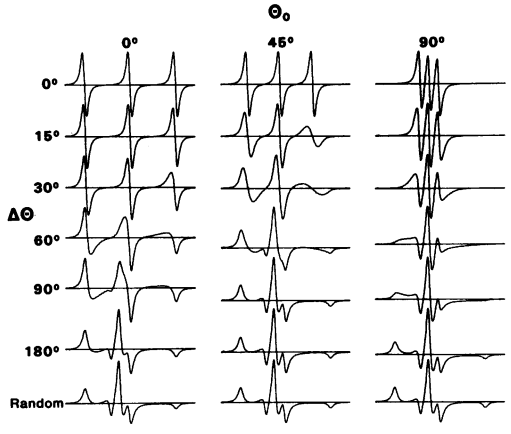


FIGURE 1 Computer-simulated spectra showing the dependence of the conventional ($V_1$) EPR spectra on $\theta_0$ (the center of the orientational distribution) and $\Delta\theta$ (the full width at half maximum of a Gaussian distribution of spins about $\theta_0$; see Eq. 2). The columns represent different values of $\theta_0$ (0°, 45°, 90°), while $\Delta\theta$ is varied along each row. The spectra are first derivatives of a Lorentzian line with half width at half maximum of 2.35 G, simulated using the following tensor values $g_\parallel = 2.00241$; $g_\perp = 2.00741$; $T_\parallel = 35.0$ G; and $T_\perp = 7.0$ G. The spectra have been normalized to the same total amplitude and are centered at 3,400 G with a scan range of 100 G.



BIOPHYS. J. © Biophysical Society · 0006-3495/86/01/144/03 $1.00
Volume 49 January 1986 144–146

contrast, variation of $\theta_0$ causes large changes in the splitting, as can be seen by comparing columns. Thus $\theta_0$ and $\Delta\theta$ can be determined independently.

## RESULTS AND DISCUSSION

From the many possible ways to determine the spectral parameters in Fig. 1, we have chosen the distance between baseline crossing points of the derivative spectrum ($2T'$) to represent the splitting, and the relative peak amplitudes (L/C) to reflect broadening effects. (The amplitude is more sensitive to linewidth change than is a direct measurement of the peak-to-peak width.) These parameters are well defined in the experimental spectra of fibers oriented parallel to the magnetic field and minimize the

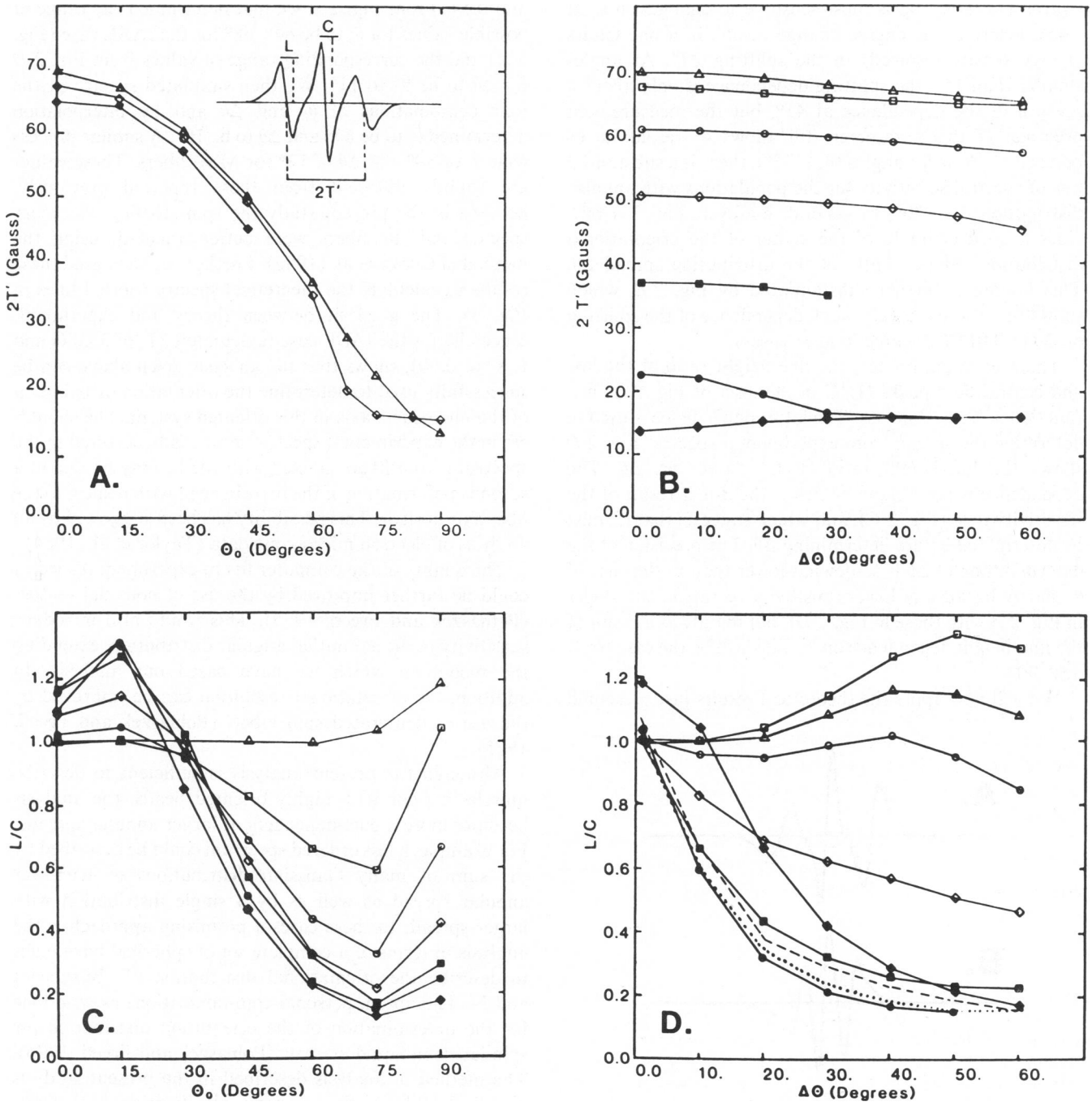


FIGURE 2 Dependence of the spectral splitting and amplitude ratio upon the orientational distribution of spins. The splitting parameter $2T'$ and the line height ratio L/C are defined in the inset Fig. 2 *A*. (*A*) $2T'$ vs $\theta_0$ for different values of $\Delta\theta$: 0° (△), 30° (◇), 60° (♦). (*B*) $2T'$ vs $\Delta\theta$ for different values of $\theta_0$: 0° (△), 15° (□), 30° (○), 45° (◇), 60° (■), 75° (●), and 90° (♦). (*C*) L/C vs. $\theta_0$ for different values of $\Delta\theta$ 0° (△), 10° (□), 20° (○), 30° (◇), 40° (■), 50° (●) and 60° (♦). (*D*) L/C vs. $\Delta\theta$ for different values of $\theta_0$: 0° (△), 15° (□), 30° (○), 45° (◇), 60° (■), 75° (●), 90° (♦), and for the best fit values of $\theta_0$ from Fig. 3, 67° (dotted line) and 80° (dashed line).

contribution of weakly immobilized or nonoriented spin populations arising from nonspecific labeling. For spectra with a large angular spread, the baseline crossing points become less well-defined, and analysis requires either the use of other spectral parameters or simulation of the entire spectrum.

Fig. 2 *A* shows the dependence of the splitting $2T'$ on the angle $\theta_0$. The splitting $2T'$ is defined in the inset to the figure. This splitting is most sensitive to changes in $\theta_0$ at ~45°, where a one degree change results in a one Gauss change (easily resolved) in the splitting $2T'$. At angles smaller than 15°, the splitting dependence is only about a seventh of the dependence at 45°, but the measurement precision of this parameter still allows 4° resolution or better in $\theta_0$. At large angles ($\theta_0 \geqq 75°$), there is a substantial loss of spectral sensitivity for the populations with angular distribution $\Delta\theta > 20°$. In general, however, Fig. 2 *A* provides a good estimate of the center of the orientational distribution independently of the distribution spread $\Delta\theta$. This finding is further substantiated by Fig. 2 *B*, which shows that there is a very weak dependence of the splitting on $\Delta\theta$ (~0.016 G/degree in most cases).

The second parameter, the line-height ratio of the low and central field peaks (L/C in the inset of Fig. 2 *A*) is a function of both $\theta_0$ and $\Delta\theta$. The latter dependence is used to determine the spread from experimental spectra. Fig. 2 *D* shows the line-height ratio (L/C) curves vs. $\Delta\theta$. The dependence is not unique, which is the direct result of the sensitivity to $\theta_0$ (Fig. 2 *C*), and which suggests that $\theta_0$ must be determined before determining $\Delta\theta$. The precision of the determination of $\Delta\theta$ is somewhat lower than in the case of $\theta_0$, partly because of lower sensitivity (compare the slopes in Fig. 2 *A* with those in Fig. 2 *D*), but mainly as a result of the line-height dependence on $\theta_0$. This will be the case for $\theta_0$ near 90°.

We will now apply the theoretical results just presented to an experimental case, oriented muscle fibers (spin-labeled as in Thomas and Cooke, 1980) in which the fiber axis is parallel to the magnetic field. The experimental spectra for two different spin labels are presented in Fig. 3 (solid lines). In each case, the spectrum contains only three well-defined lines, suggesting that the analysis of Fig. 2 can be applied. The parameter $2T'$ was 29.6 G and 17.0 G for IASL- and MSL-labeled psoas fibers, and L/C was 0.62 and 0.54. From Fig. 2 *A* we first determined the range of possible values for $\theta_0$ to be 64°–68° for the IASL case (Fig. 3 *A*) and the corresponding range of values from Fig. 2 *D* for $\Delta\theta$ to be 9° to 11°. We then simulated spectra at the four combinations of $\theta_0$ and $\Delta\theta$ and by interpolation determined $\theta_0$ to be 67° and $\Delta\theta$ to be 10°. A similar process gave $\theta_0$ of 80° and $\Delta\theta$ of 13° for MSL fibers. These values are slightly different from those reported previously, because in the present study the spin-labeling was more specific and the fibers were better oriented, using the method of Cooke et al. (1982). Further, we then used these results to calculate the theoretical spectra (dotted lines in Fig. 3). The good fit between theory and experiment, especially for the IASL case (calculated $2T'$ of 30.0 G and L/C of 0.60), shows that the analysis given above can be successfully used to determine the orientation distribution of the nitroxide $\hat{z}$ axis in this oriented system. The shoulders in the experimental spectra, most easily detected in the spectrum from fibers labeled with MSL, may be due to a second conformation of the myosin head with respect to the fiber axis in rigor. This possibility has been suggested by an analysis of electron microscopy data (Taylor et al., 1984).

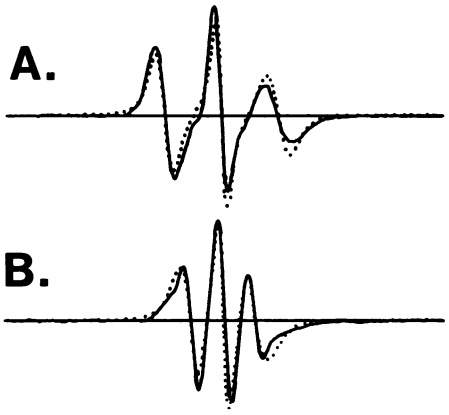


FIGURE 3 Comparison of experimental (solid line) and simulated spectra (broken line) for muscle fiber bundles oriented parallel to the magnetic field $H_0$. Spin labels were attached selectively to $SH_1$ on the myosin heads. (*A*) Iodoacetamide spin label (IASL): $\theta_0 = 67°$, $\Delta\theta = 10°$, and (*B*) maleimide spin label (MSL): $\theta_0 = 80°$, $\Delta\theta = 13°$. Other experimental details can be found in Thomas and Cooke (1980).

The quality of the computer fits to experimental spectra could be further improved by the use of nonaxial tensors (Polnaszek and Freed, 1975). This would also introduce sensitivity to the azimuthal angular distribution, extending the model on which we have based our analysis. In addition, the orientational resolution can be improved by the use of deuterated spin labels (Polnaszek and Freed, 1975).

Although the present analysis is sufficient to describe muscle in rigor with highly oriented heads, the analysis becomes more model-dependent at larger angular spreads. For example, a less ordered spectrum could be described by the sum of many Gaussian distributions of narrower angular spread as well as by a single distribution with larger spread. In these cases a promising approach is the analysis in terms of a complete set of spherical harmonics to describe the orientational distribution (T. Burghardt and N. Thompson, personal communication) as was done for the determination of the orientation distribution for spin labels in liquid crystals (Polnaszek and Freed, 1975). The method of analysis described in the present study is also applicable to other macroscopically oriented systems, such as a stack of oriented membranes in which the membrane normal replaces the fiber axis in the analysis.

We thank Roger Cooke, Mark Crowder, Jeffrey Lu, Christine Wendt, and Eric Svensson for helpful discussions.

This work was supported by grants from the National Institutes of Health (GM 27906 and AM 32961), the American Heart Association (80-850), the National Science Foundation (PCM 8004612), and the Muscular Dystrophy Association of America. D. D. Thomas is an Established Investigator of the American Heart Association, P. Fajer is a Muscular Dystrophy Postdoctoral Fellow, and V. A. Barnett is a National Science Foundation Predoctoral Fellow.

*Received for publication 4 June 1985.*

## REFERENCES

Barnett, V. A., and D. D. Thomas. 1984. Saturation transfer EPR of spin-labeled muscle fibers: dependence on sarcomere length. *J. Mol. Biol.* 179:83–102.

Cooke, R., M. S. Crowder, and D. D. Thomas. 1982. Orientation of spin-labeled myosin heads in contracting muscle fibers. *Nature (Lond.)*. 300:776–778.

Heuser, J. G. 1983. Direct visualisation of the myosin cross-bridge helices on relaxed rabbit psoas thick filaments. *J. Mol Biol.* 171:105–109.

Huxley, H. E., and W. Brown. 1967. The low angle x-ray diagram of vertebrate striated muscle and its behaviour during contraction and rigor. *J. Mol. Biol.* 30:383–434.

Polnaszek, C. F., and J. H. Freed. 1975. ESR studies of anisotropic ordering, spin relaxation and slow tumbling in liquid crystalline solvents. *J. Phys. Chem.* 79:2283–2306.

Poulsen, F. R., and J. Lowy. 1983. Small-angle x-ray scattering from myosin heads in relaxed and rigor frog skeletal muscles. *Nature (Lond.)*. 207:146–152.

Taylor, K. A., M. C. Reedy, L. Cordova, and M. K. Reedy. 1984. Three-dimensional reconstruction of rigor insect flight muscle from tilted thin sections. *Nature (Lond.)*. 310:285–291.

Thomas, D. D., and R. Cooke. 1980. Orientation of spin-labeled myosin heads in glycerinated muscle fibers. *Biophys. J.* 32:891–906.

Thomas, D. D., S. Ishiwata, J. C. Seidel, and J. Gergely. 1980. Submillisecond rotational dynamics of spin-labeled cross-bridges in myofibrils. *Biophys. J.* 32:873–890.

# ASSEMBLY OF ACTIN FILAMENTS STUDIED BY LASER LIGHT SCATTERING AND FLUORESCENCE PHOTOBLEACHING RECOVERY

BENNIE R. WARE AND JAMES W. KLEIN
*Department of Chemistry, Syracuse University, Syracuse, New York 13210*

One of the most fascinating macromolecular assemblies found in nature is the contractile apparatus responsible for cytoplasmic motility. All living cells possess the capacity for generating directed force to accomplish active motion. This capacity is manifest in a number of fundamental cellular functions such as cell division, secretion, phagocytosis, and locomotion. Despite over three centuries of fascination with cytoplasmic motility, the molecular mechanism of force generation is still a subject of more conjecture than understanding. Though analogies with the mechanism of the contraction of skeletal muscle are compeling and often instructive, the essential difference is the absence of a static structure in the cytoplasm. The transient assembly of a fragile molecular apparatus for force generation in the cytoplasm must require a complicated and dynamic regulation of even greater subtlety than its counterpart in muscle; and a study of the structure and dynamics of the transient assembly responsible for cytoplasmic contractility will surely require an even wider range of sophisticated physical techniques.

It is agreed that the primary structural component of the cytoplasmic contractile apparatus is actin. Cytoplasmic actin is virtually identical to the actin of skeletal muscle, and the self-assembly of cytoplasmic globular actin (G-actin) to actin filaments (F-actin) appears to be a fundamental event of cytoplasmic motile processes (1). In addition, there are a host of proteins in the cytoplasm whose role seems to be regulation of the assembly and cross-linking of actin filaments into a supramolecular network capable of generating force, presumably by interaction with cytoplasmic myosin. Because of the transience, fragility, and complexity of the supramolecular complex associated with cytoplasmic motility, the common structural techniques that have been successful in studying other macromolecular assemblies are often inappropriate for addressing the fundamental issues of the structure and function of the cytoplasmic contractile network.

Our research group has addressed itself to the study of the supramolecular complexes associated with cytoplasmic motility by the measurement of transport coefficients in simple solutions, in complex mixtures, and in native cytoplasm. The transport coefficients measured are (*a*) the mutual diffusion coefficient in solution, which we measure by quasi-elastic light scattering (QELS) (2, 3); (*b*) the tracer diffusion coefficient either in solution or in complex mixtures, which we measure by fluorescence photobleaching recovery (FPR) (4); and (*c*) the electrophoretic mobility in solution, which we measure by electrophoretic light scattering (5). These transport coefficients can be used to characterize the molecular dimensions and electrical charge of the components of the cytoplasmic supramolecular complexes and, in some cases, are able to provide pertinent information regarding the association of specific components with the assemblies and/or the mobility of specific components or probe particles within and through the assembled networks.